Journal of Solid State Chemistry 184 (2011) 2770–2775

Contents lists available at SciVerse ScienceDirect

Journal of Solid State Chemistry

journal homepage: www.elsevier.com/locate/jssc

Microstructures and photocatalytic properties of Ag^+ and La^{3+} surface codoped TiO_2 films prepared by sol–gel method

Nan Zhao [a], Ming-ming Yao [a,*], Fang Li [a], Fei-peng Lou [b]

[a] Key Laboratory of Chemical Sensing & Analysis, Universities of Shandong, School of Chemistry and Chemical Engineering, University of Jinan, Jinan 250022, China
[b] China Petroleum Engineering & Construction Corporation, Beijing 100120, China

ARTICLE INFO

Article history:
Received 24 May 2011
Received in revised form
21 July 2011
Accepted 10 August 2011
Available online 19 August 2011

Keywords:
Sol–gel
TiO_2 film
Ag^+/La^{3+} codoping
Surface doping
Photocatalytic activity

ABSTRACT

Ag^+ and La^{3+} surface codoped TiO_2 films were successfully prepared by the improved sol–gel and doping processes. The as-prepared specimens were characterized using differential thermal analysis-thermogravimetry (DTA–TG), X-ray diffraction (XRD), high-resolution field emission scanning electron microscopy (FE-SEM), X-ray energy dispersive spectroscopy (EDS), Brunauer–Emmett–Teller (BET) surface area, Photoluminescence spectrum (PL) and UV–vis diffuse reflectance spectroscopy. The photocatalytic activities of the films were evaluated by degradation of an organic dye in aqueous solution. The results of XRD, FE-SEM and BET analyses indicated that the TiO_2 films were composed of nano-particles or aggregates with a size of less than 10 nm. With the codoping of Ag^+ and La^{3+}, TiO_2 films with high photocatalytic activity and clearly responsive to the visible light were obtained. The improvement mechanism by ions doping was also discussed.

1. Introduction

Semiconductor heterogeneous photocatalytic oxidation process is a popular technique that has great potential to control aqueous organic contaminates or air pollutants [1,2]. These processes are all characterized by the same chemical features such as production of hydroxyl radicals (OH) and superoxide anion (O^{2-}), which are generated when a semiconductor catalyst absorbs radiation when it is in contact with water and oxygen. Among various oxide semiconductor photocatalysts, TiO_2 photocatalysis is considered as an attractive approach because of its strong oxidizing power, photo-stability, non-toxicity, chemical and biological inertness, as well as its low cost [3–7]. However, conventional powdered TiO_2 is limited as photocatalysts, since a post-treatment separation is required to recover the catalyst in wastewater treatment process. Nano-oxide films with a great potential for applications have attracted considerable interests recently.

The photocatalytic activity of the TiO_2 is due to the production of photo-generated electrons (e^-) and corresponding positive holes (h^+) under UV illumination. However, the species are unstable, and the recombination of electrons and holes can occur very quickly. In fact, the photocatalytic efficiency of TiO_2 to degrade pollutants decreases substantially due to the high recombination ratio of the species. To reduce the recombination of photo-generated electrons and holes, and to extend the light absorption of TiO_2 into visible light region, many approaches have been carried out including various preparation, different carriers, surface modifications, etc. The introduction of transition metal ions in the photocatalytic reaction is one of the most efficient and simplest way of surface modification. Among the transition metal ions studies, silver ions doping has been the most interesting one due to the remarkable improvement of the photocatalytic activity of TiO_2. Seery et al. [8] reported silver doped titanium dioxide nanomaterials prepared by the sol–gel process, and tests found that the Ag doping could enhance the photocatalytic activities of TiO_2 materials under visible light. Serrano et al. [9] prepared TiO_2 nanoparticles doped with different Ag contents by a modified sol–gel method, and tests found that the Ag doping could increase the thermal stability of the TiO_2 particles, enhance the crystallization process, and inhibit the normal anatase-rutile phase transition when annealed in air. Ao et al. [10] synthesized Ag-doped mesoporous titania via a combined sol–gel process with surfactant-assisted templating method, and tests found that the sample with 0.5% Ag doping had the highest photocatalytic activity. Moreover, modification of TiO_2 nanoparticles or nanofilms through a small amount of lanthanide metals is also increasingly being considered for maximizing its photocatalytic efficiency due to the distinctive chemical, physical and electronic features of lanthanide metals. Wu et al. [11] prepared enhanced photocatalytic activity of TiO_2 films with doped La by micro-plasma

* Corresponding author. Fax: +86 531 82765969.
E-mail addresses: yaomm4364@sina.com, chm_yaomm@ujn.edu.cn (M.-m. Yao).

0022-4596/$ - see front matter © 2011 Elsevier Inc. All rights reserved.
doi:10.1016/j.jssc.2011.08.014

oxidation method, and suggested that the enhanced photocatalytic activities might be related to the forming of titanium dioxide lattice distortion, which might be easy to accumulate variable oxygen vacancy so as to trap photo-generate holes.

Compared with the conventional method of ions doping, we adopted a simple sol–gel process to prepare Ag^+ and La^{3+} surface codoped TiO_2 films in this paper. To the best of our knowledge, there were few study concentrated on Ag and La modified TiO_2 films for the photodegradation of organic dyes in aqueous solutions, and the effects of ions doping on photocatalytic activity and microstructures of TiO_2 films have not been reported.

2. Experimental

All chemicals used in this study were of analytical reagent grade quality. Double-distilled deionized water was used throughout.

Colloidal TiO_2 was prepared by the simple sol–gel method. A total volume of 1 ml $TiO(C_4H_9O)_4$ was dissolved in 20 ml ethanol absolute under vigorous stirring in a clean and dry vessel at room temperature. After 5 min, 20 ml diluted nitric acid (0.2 M) was added to the above solution at the speed of 1 drop/s and kept on stirring till the colloidal suspension could be obtained. Colloidal TiO_2 films were coated to the surface of glass substrate (25 mm × 25 mm × 1 mm) by a controllable dip-coating device in an ambient atmosphere. The speed was controlled at 3 mm s^{-1}. After a dip-coating for different times, the TiO_2 sol- or gel-film for different thickness was obtained. A certain concentration of silver nitrate ($AgNO_3$) or lanthanum nitrate ($La(NO_3)_3$) aqueous solution was doped onto the surface layer of TiO_2 gel-film, which should be called external doping or surface doping. Then, the ions doped TiO_2 gel-films on glass substrate were calcined in air at a rate of 5 °C/min up to 450 °C and were left to stay in the furnace for 1 h for organics removal and crystalline TiO_2. Normally, ions were directly doped into TiO_2 sol precursor, which should be called internal doping or bulk doping.

The thickness of TiO_2 film can be approximately calculated by formula: $H=W_2-W_1/\rho ld$, in which H is the thickness of film, W_1 is the weight of glass substrate before coated film while W_2 after it, ρ is the density of TiO_2, l and d are the length and width of substrate, respectively. In our experiments, the thickness of TiO_2 film was 1.20 μm ± 5%, and doping ions extended into the film less than 50 nm deep determined by X-ray photoelectron spectroscopy.

The crystallization behavior the TiO_2 was monitored using a differential thermal analysis-thermogravimetry (DTA–TG) machine. The identity of crystalline phase and the crystallite size of the TiO_2 samples were identified by X-ray diffraction with a diffractometer employing Cu $K\alpha$ radiation at a scan rate (2θ) of 0.05° S^{-1}. The accelerating voltage and the applied current were 40 kV and 25 mA, respectively. Surface morphology of the TiO_2 films was characterized by high-resolution field emission scanning electron microscopy (FE-SEM). The Brunauer–Emmett–Teller (BET) surface area of the TiO_2 samples was analyzed by nitrogen adsorption/desorption apparatus. The surface area was determined by the multipoint BET method using the adsorption data in the relative pressure (P/P_0) range of 0–1.0, and the desorption isotherm was used to determine the pore size distribution using the Barret–Joyner–Halender (BJH) method. The nitrogen adsorption volume at the relative pressure (P/P_0) of 0.975 was used to determine the pore volume and average pore size. The recombination of electron–hole in the samples was studied by photoluminescence emission spectra, which was measured on a luminescence spectrometer (FLS 920).

The photocatalytic efficiency was evaluated by the degradation of Acid Naphthol Red (ANR) in an aqueous solution under both UV and visible light irradiations. Metal ions doped or undoped TiO_2 films were settled in 5 ml aqueous organic dyes with a concentration of 1.0×10^{-4} mol dm^{-3} in a weighing bottle. A 300 W tungsten halogen lamp equipped with a UV cut-off filters ($\lambda>400$ nm) was used as a visible light source, and the wavelength of 365 nm was used as a UV light source. In our experiments, the volume of ions doping solution was fixed to 0.05 ml, while the concentration of ions doping solution was changeable. The measurements were repeated for each catalytic system, and the experimental error was found to be within the acceptable limit (± 5%). Their photocatalytic degradation rate can be calculated by formula: $D=(A_0-A)/A_0\times100\%$, in which A_0 is the absorbency of the organic dye solution before illumination while A after it.

3. Results and discussion

The typical DTA–TG curves of TiO_2 samples are shown in Fig. 1. On the DTA curve, a broad endothermic peak at below 150 °C is due to dehydration, and two relatively small exothermic peaks at 217.0 °C and 290.1 °C, respectively, are due to combustion of organic substances contained in the gel. Of course, the positions and intensities of the peaks are strongly dependent on the gel preparation process and its composition. At 387.7 °C a very small exothermic peak observed may be due to the transformation of TiO_2 from amorphous to crystalline existed in the form of anatase with a little brookite, and at about 504.1 °C brookite phase disappears. The temperature of the phase transition from anatase to rutile is at 542.2 °C. Therefore, rutile is a stable phase at high temperature, while anatase and brookite are metastable phases. In addition, from the TG curve we can clearly see that the curve becomes almost straight line at about 450 °C, indicating organic substances has been completely burned. On the basis of the DTA–TG curves analyses, all TiO_2 samples calcined at 450 °C in air for 1.0 h in our experiments.

Normally, the anatase phase of titania is the main product in hydrolytic sol–gel synthesis of nanocrystalline titania. However, brookite or rutile is often present as a byproduct. Fig. 2 shows the XRD spectra of the undoped and ions doped TiO_2 samples calcined at 450 °C in air for 1.0 h. The samples exhibit a good crystallinity constituted of a mixture of anatase (25.6°, 37.8°, 48.3°), rutile (27.6°, 36.1°) and brookite (30.9°), but the anatase phase is dominant in the as-prepared TiO_2 samples. From Fig. 2, it can

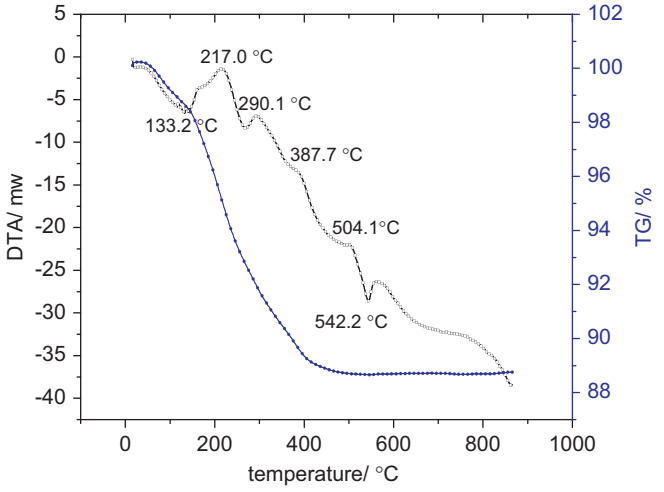

Fig. 1. A typical DTA–TG curves of TiO_2 samples.

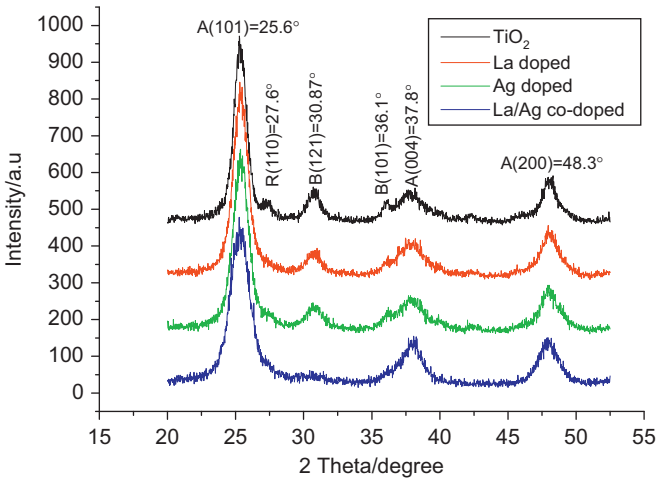

Fig. 2. XRD patterns of pure TiO_2 and ions doped TiO_2.

be seen clearly that the rutile peaks of TiO_2 samples have disappeared after Ag^+ or La^{3+} single doping and Ag^+/La^{3+} codoping, while the intensity of brookite peaks have become weaker after Ag^+ or La^{3+} single doping, even disappeared after Ag^+/La^{3+} codoping, indicating that ions doping cannot only suppress the formation of brookite phase but also inhibit the transformation of anatase to rutile at high temperature. According to the Scherrer equation: $D=0.89\lambda/\beta\cos\theta$, where β is the half-height width of the diffraction peak of anatase, θ is the diffraction angle, and λ is the X-ray wavelength corresponding to the Cu $K\alpha$ radiation, we can calculate that the average size of pure TiO_2 particles is 6.5 nm, compared with 5.6 nm of Ag^+ and La^{3+} codoped TiO_2. The well-crystallized TiO_2 anatase can facilitate the transfer of the photo-induced electron, and lower the probability of recombination of photo-induced holes and electrons. Based on the XRD analyses, Ag^+ and La^{3+} codoping can inhibit the phase transformation of TiO_2 in the solid and hinder the increase of the crystallite size, which can result in the higher photocatalytic activity of the TiO_2 samples.

Surface morphology of pure TiO_2 films and Ag^+ and La^{3+} codoped TiO_2 films calcined at 450 °C in air for 1.0 h are shown in Fig. 3. It is clear that the films are composed of round-like nanoparticles or aggregates with a size of less than 10 nm, and indicating that the surface of the Ag^+ and La^{3+} codoped TiO_2 films is relatively uniform and smooth without cracks. A good dispersion among particles may increase the active site-reactant contact area, and enhance photocatalytic degradation of organic dyes. EDS element analyses indicate that the atomic ratio of Ti/O/Ag/La in codoped TiO_2 is 26.92/71.25/0.32/1.51.

N_2 adsorption/desorption isotherms of pure TiO_2 samples and Ag^+ and La^{3+} codoped TiO_2 samples calcined at 450 °C in air for 1.0 h are shown in Fig. 4a. From Fig. 4a, we can know that the isotherms of the two samples exhibit hysteresis loops at high relative pressures from 0.4 to 0.8. The sharp decline in desorption curve is indicative of mesoporosity, while the hysteresis loop demonstrates that there exists bottle-neck mesoporous structure, possibly caused by non-uniform pore size. It is evident that with the same relative pressure codoped TiO_2 samples have higher adsorption quantities as well as higher surface area. In our experiment, specific surface area of Ag^+ and La^{3+} codoped TiO_2 sample is 130.9 $m^2\,g^{-1}$, more than that of pure TiO_2 sample 109.6 $m^2\,g^{-1}$.

The pore sizes distributions of the as-prepared samples are shown in Fig. 4b, indicating that the pores with size less than 4 nm reach as high as 94.26% after Ag^+ and La^{3+} codoped TiO_2 compared with 90.35% of undoped TiO_2, while the ones with size

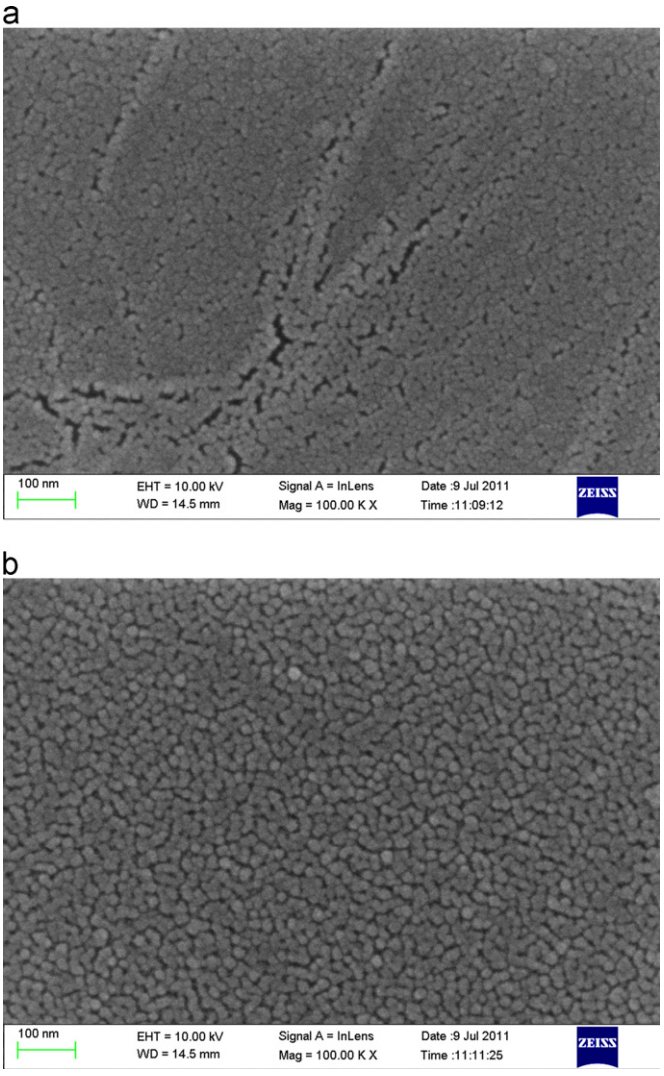

Fig. 3. FE-SEM images for TiO_2 samples: (a) Pure TiO_2 film and (b) Ag^+ and La^{3+} codoped TiO_2 film.

more than 4 nm are only 5.73% after Ag^+ and La^{3+} codoped TiO_2 compared with 9.65% of undoped TiO_2. It is evident that Ag^+ and La^{3+} codoping can decrease the pore sizes of the TiO_2 samples. The smaller pores and the larger specific surface area of the TiO_2 samples by Ag^+ and La^{3+} codoping are favorable to the photocatalytic degradation.

The recombination of electron–hole in the TiO_2 samples was studied by photoluminescence emission spectra [12]. The PL emission spectra of three samples were recorded in the wavelength range of 300–600 nm in our study, as shown in Fig. 5. It can be observed that the position of the peaks about 380 nm due to the emission of the band gap transition were similar while PL intensities were quite different among three samples. The PL intensity of Ag^+/La^{3+} surface codoped TiO_2 was the lowest among all samples, indicating the recombination of electron and hole was effectively prohibited compared with pure TiO_2, Ag^+/La^{3+} bulk codoped TiO_2. It is well-known the photocatalytic efficiency depends on the competition between the surface charge carrier transfer rate and the electron–hole recombination rate. Charge trapping by bulk doped ions consumed large quantities of charge carriers before their diffusion to the surface (deep trapping), thus reducing the activities of the bulk doped ions samples. In contrast to bulk doped TiO_2 samples, surface doping allows most of charge carriers to successfully migrate to the surface and prevents

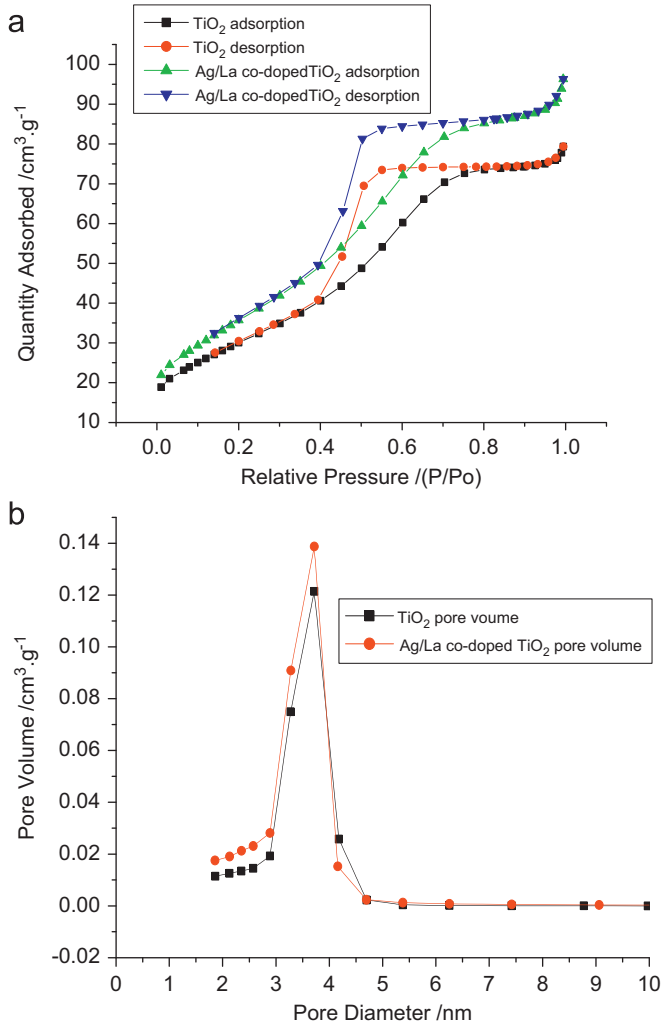

Fig. 4. N_2 adsorption/desorption isotherms (a) and pore size distribution (b) of pure TiO_2 and Ag^+/La^{3+} codoped TiO_2.

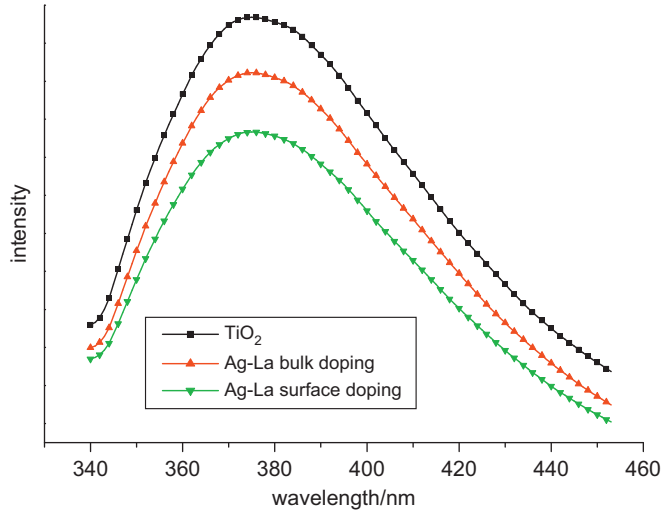

Fig. 5. Effect of ions doping modes on PL spectra.

surface recombination for high photocatalytic activities [13]. In our experiments, the degradation rate of aqueous ANR using surface codoping Ag^+/La^{3+} TiO_2 film is 62.5%, compared with that of bulk codoping Ag^+/La^{3+} TiO_2 film 55.3% under the same conditions. Therefore, we adopted a surface doping process to prepare ions doped TiO_2 film in following experiments.

Fig. 6 shows UV–vis absorption spectra (a) and degradation rate (b) of ANR solutions using an appropriate amount of Ag^+, La^{3+}, Ag^+/La^{3+} doped and undoped TiO_2 films on glass substrates under UV-lamp irradiation with wavelength of 365 nm for 45 min. From Fig. 6, it can be seen that the degradation rates of aqueous ANR using TiO_2 film is 33.5%, compared with that of Ag^+ doped TiO_2 film 53.9%; La^{3+} doped TiO_2 film 54.2%; and Ag^+ and La^{3+} codoped TiO_2 films 62.5%. Obviously, we can draw the conclusion that Ag^+ and La^{3+} codoped TiO_2 films have the best photocatalytic activity under the same conditions. Since the ions dopant can serve not only as a mediator of interfacial charge transfer but also as a recombination center, the photocatalytic activity of ions doped TiO_2 is strongly dependent on the dopant concentration. In our case, an optimal Ag^+ or La^{3+} doping concentration is 7×10^{-3} M, while an optimal co-doping concentration is Ag^+ 1×10^{-3} M, La^{3+} 6×10^{-3} M.

Diffuse reflection UV–vis spectra of undoped and Ag^+/La^{3+} codoped TiO_2 film are shown in Fig. 7. It is clear that the absorbance onset of codoped TiO_2 film red shift obviously to about 450 nm compared with that of pure TiO_2 film 350 nm. It is worth mentioning that Ag^+/La^{3+} codoped TiO_2 film has

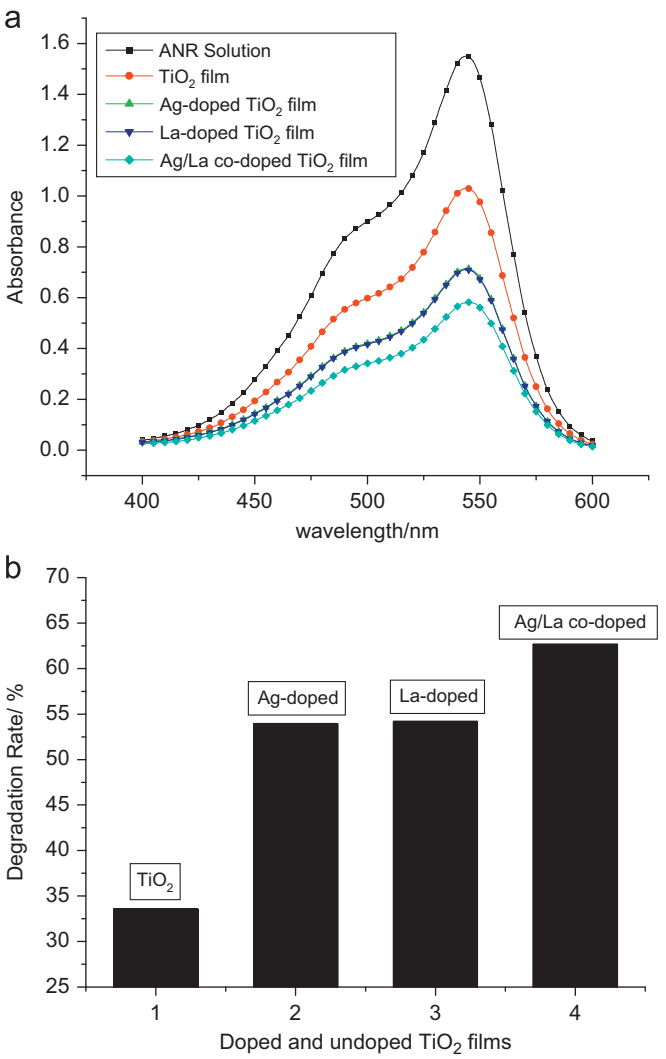

Fig. 6. UV–vis absorption spectra (a) and degradation rate (b) of ANR solutions using an appropriate amount of Ag^+, La^{3+}, Ag^+/La^{3+} doped and undoped TiO_2 films on glass substrates after irradiated for 45 min.

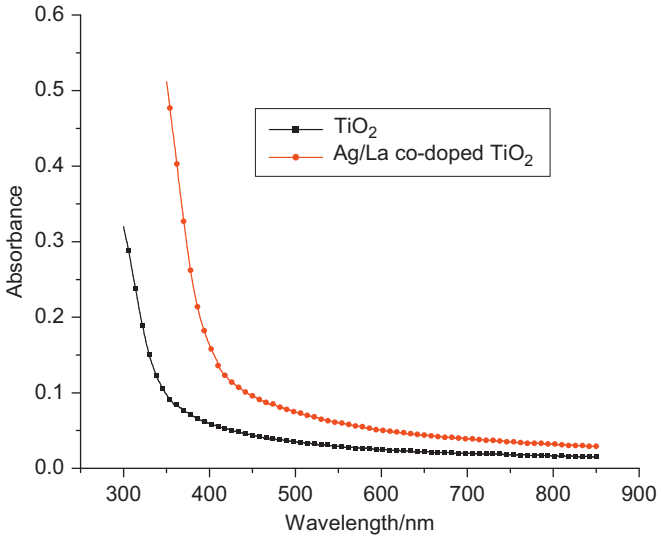

Fig. 7. Diffuse reflection UV–vis spectra of undoped and Ag^{+}/La^{3+} doped TiO_2 film.

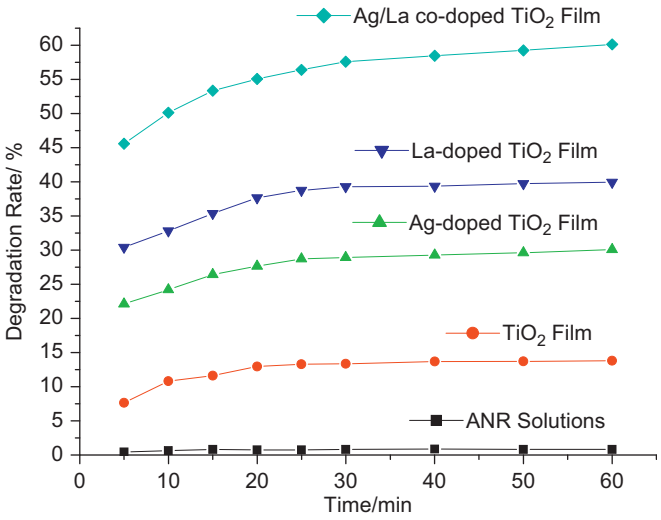

Fig. 8. Degradation rate of ANR solutions using undoped and doped TiO_2 films after visible light irradiated for 60 min.

a remarkably higher absorption in the visible region with respect to pure TiO_2 film.

Fig. 8 shows the degradation rate of ANR solutions using an appropriate amount of Ag^{+}, La^{3+}, Ag^{+}/La^{3+} doped and undoped TiO_2 films on glass substrates after visible light irradiated for 60 min. From Fig. 8, the degradation rate of ANR using TiO_2 film is about 13.8%, compared with that of Ag^{+} doped TiO_2 film 30.1%, La^{3+} doped TiO_2 film 39.9%, and Ag^{+}/La^{3+} codoped TiO_2 film 60.1%, while the ANR solutions without TiO_2 film have almost no photo-degradation.

Based on the above experiments, Ag^{+} and La^{3+} surface codoped TiO_2 films exhibit excellent photocatalytic activity under both UV and visible light irradiations. This may be ascribed to the fact that the microstructure of TiO_2 films and the effect of the doping modes. First of all, the surface microstructure, including morphology of surface, grain size and crystalline phase of TiO_2, pore size and distribution, and so on, is of great influence on the photocatalytic activity of TiO_2 films. According to the above, FE-SEM, XRD and BET analyses, Ag^{+} and La^{3+} codoping can effectively lessen the aggregation of the TiO_2 nano-particles, induce the pores uniform, decrease the numbers of micro-pores, and increase specific surface area of the TiO_2 films, as well as inhibit the transformation of anatase to rutile. These factors lead to effective photodegradation of organic dyes. Secondly, surface doping improve the photocatalytic activity of TiO_2 film to a greater extent than does bulk doping, because surface doping allows most of charge carriers to successfully migrate to the surface and prevents surface recombination. Meanwhile, Ag^{+}/La^{3+} codoping is more beneficial than single doping to the photocatalytic activity of TiO_2 film, because Ag^{+} and La^{3+} codoping can effectively reduce the recombination of photo-generated electrons and holes. On one hand, Ag^{+} ions doping can result from formation of dopant energy level within the band gap of TiO_2, leading to more photo-generated carriers to join in the degradation reaction. On the other hand, Ag^{+} doping can also reduce the recombination of photo-generated electrons and holes through trapping electrons. It is well-known that Ag^{+} ion has a completely filled d orbital and empty s orbital ($4d^{10}5s^{0}$), which is relatively stable, and electrons trapped can be easily released, so it elongates the life of photo-excited electrons and holes. Normally, the La^{3+} does not form any impurity level in the forbidden band of TiO_2, but La^{3+} ions doping can lead to the formation of titanium dioxide lattice distortion, which is easy to accumulate variable oxygen vacancy so as to trap photo-generate holes [14]. Moreover, La^{3+} ion has a completely empty orbital ($4f^{0}5d^{0}6s^{0}$), which is also relatively stable, and holes trapped can be easily released, so it elongates the life of photo-excited electrons and holes. The major steps in the mechanism may be summarized by Eqs. (1)–(8) [15].

$$TiO_2 + h\nu \rightarrow h^{+} + e^{-} \quad (1)$$

$$Ti^{4+} + e^{-} \rightarrow Ti^{3+} \quad (2)$$

$$O^{2-} + h^{+} \rightarrow O^{-} \quad (3)$$

$$Ag^{+} + Ti^{3+} \rightarrow Ag^{0} + Ti^{4+} \text{ electron trap} \quad (4)$$

$$La^{3+} + O^{-} \rightarrow La^{4+} + O^{2-} \text{ hole trap} \quad (5)$$

$$La^{4+} + OH^{-} \rightarrow La^{3+} + OH \text{ hole release} \quad (6)$$

$$2Ag^{0} + O_2 \rightarrow 2Ag^{+} + O^{2-} \text{electron release} \quad (7)$$

$$\text{Dye} + O^{2-} \text{ or } OH \rightarrow \text{the degraded products} \quad (8)$$

In a word, If the amount of Ag^{+}/La^{3+} codoping is appropriate, the photocatalytic activity of the TiO_2 film can significantly enhance. Moreover, small addition of rare earth metals, such as La, etc., can reduce the number of pores produced at the film/substrate interface, enhancing the adherence of the TiO_2 films to the substrates, and therefore being favorable to photocatalytic activity after a long time exposure to air [16].

4. Conclusions

Our experimental results confirmed that ions surface doping significantly improved the photodegradation of organic dyes with respect to ions bulk doping. The obvious red shift of absorption edge of TiO_2 films by ions surface codoping may promise a potential application for TiO_2 films in visible light. Moreover, modified TiO_2 films can set a good ground for the design and development of efficient continuous flow photocatalytic reactors.

Acknowledgments

This work was financially supported partially by National Natural Science Foundation of China (Grant no. 20674005) and the Doctorial Foundation of University of Jinan (B0606).

References

[1] S. Ahmed, M.G. Rasul, W.N. Martens, R. Brown, M.A. Hashib, Water Air Soil Pollut. 215 (2011) 3–29.
[2] A. Zaleska, E. Grabowska, J. Sobczak, M. Gazda, J. Hupka, Appl. Catal. B 89 (2009) 469–475.
[3] Y.X. Rao, D.M. Antonelli, J. Mater. Chem. 19 (2009) 1937–1944.
[4] Y. Huang, G. Xie, S.P. Chen, S.L. Gao, J. Solid State Chem. 184 (2011) 502–508.
[5] Y.M. Wu, J.L. Zhang, L. Xiao, F. Chen, Appl. Catal. B 88 (2009) 525–532.
[6] J.C. Yu, W. Ho, J. Yu, H. Yip, P.K. Wong, J. Zhao, Environ. Sci. Technol. 39 (2005) 1175–1179.
[7] H.J. Zhang, G.H. Chen, D.W. Bahnemann, J. Mater. Chem. 19 (2009) 5089–5121.
[8] M.K. Seery, R. George, P. Floris, S.C. Pillai, J. Photochem. Photobiol. A 189 (2007) 258–263.
[9] J. García-Serrano, E. Gómez-Hernández, M. Ocampo-Fernández, U. Pal, Curr. Appl. Phys. 9 (2009) 1097–1105.
[10] Y.H. Ao, J.J. Xu, D.G. Fu, C.W. Yuan, J. Phys. Chem. Solids 69 (2008) 2660–2664.
[11] X.H. Wu, X.B. Ding, W. Qin, W.D. He, Z.H. Jiang, J. Hazard. Mater. 137 (2006) 192–197.
[12] Y.M. Wu, J.L. Zhang, L. Xiao, F. Chen., Appl. Catal. B 88 (2009) 525–532.
[13] S.M. Chang, W.S. Liu, Appl. Catal. B 101 (2011) 333–342.
[14] B. Reddy, A. Khan, Catal. Surv. Asia 9 (2005) 155–171.
[15] J.C. Yu, W. Ho, J. Liu, H. Yip, P.K. Wong, Environ. Sci. Technol. 37 (2003) 2296–2301.
[16] M.M. Yao, Y.D. He, W. Zhang, W. Gao, Mater. Trans. 46 (2005) 2089–2092.